

Monitoring concrete bridge decks using infrared thermography with high speed vehicles

Shuhei Hiasa^{1,2a}, F. Necati Catbas^{*1}, Masato Matsumoto^{3b} and Koji Mitani^{3c}

¹Department of Civil Environmental and Construction Engineering, University of Central Florida, 12800 Pegasus Drive, Suite 211, Orlando, Florida 32816, USA

²West Nippon Expressway Company Limited (NEXCO-West), Dojima Avanza 19F, 1-6-20 Dojima, Kita-ku, Osaka, 530-0003, Japan

³NEXCO-West USA Inc. 8300, Boone Blvd., Suite 240, Vienna, Virginia, 22182, USA

(Received March 5, 2016, Revised June 3, 2016, Accepted June 8, 2016)

Abstract. There is a need for rapid and objective assessment of concrete bridge decks for maintenance decision making. Infrared Thermography (IRT) has great potential to identify deck delaminations more objectively than routine visual inspections or chain drag tests. In addition, it is possible to collect reliable data rapidly with appropriate IRT cameras attached to vehicles and the data are analyzed effectively. This research compares three infrared cameras with different specifications at different times and speeds for data collection, and explores several factors affecting the utilization of IRT in regards to subsurface damage detection in concrete structures, specifically when the IRT is utilized for high-speed bridge deck inspection at normal driving speeds. These results show that IRT can detect up to 2.54 cm delamination from the concrete surface at any time period. It is observed that nighttime would be the most suitable time frame with less false detections and interferences from the sunlight and less adverse effect due to direct sunlight, making more “noise” for the IRT results. This study also revealed two important factors of camera specifications for high-speed inspection by IRT as shorter integration time and higher pixel resolution.

Keywords: infrared thermography; monitoring; non-destructive evaluation; high-speed inspection; bridge deck; delamination; IR camera specifications; cooled IR camera; integration time; pixel resolution

1. Introduction

1.1 Background

Deterioration of road infrastructure arises from aging and various other factors. Consequently, inspection and maintenance have been a serious worldwide problem, especially in developed countries such as the United States and Japan. While the number of bridges have been increasing with 610,749 bridges in the USA as of 2014 (FHWA 2014) and approximately 700,000 bridges

*Corresponding author, Professor, E-mail: catbas@ucf.edu

^a Ph.D., E-mail: hiasa615@Knights.ucf.edu

^b P.E.(JPN), E-mail: m.matsumoto@w-nexco-usa.com

^c Ph.D., E-mail: k.mitani@w-nexco-usa.com

(more than 2 m) in Japan as of 2014 (MLIT 2014), the resources to inspect and maintain those bridges are limited in both budget and personnel. The aging of bridges is one of the most critical factors for deterioration of their condition and it is obvious that as more bridges age, the number of deficient bridge will increase. In order to prevent the impending degradation of these bridges, periodic inspection and proper maintenance are indispensable.

In terms of inspection frequency in the United States, Section 1111 of the Moving Ahead for Progress in the 21st Century Act (MAP-21) (Public Law 112–141 2012) amended Section 144 of title 23, United States Code (OLRC 2012), requires each state and appropriate federal agency to report element level bridge inspection data for bridges on the National Highway System (NHS) to the FHWA on an annual basis from 2015 (FHWA 2013). On the other hand, FHWA (2013) also states that each NHS highway bridge is inspected in accordance with 23 CFR 650 Subpart C, which requires biennial inspection for each bridge (GPO 2015). Still, annual inspection is not required at the present, yet there is a possibility that bridges will be required to undergo annual inspection in accordance with the progression of aging and deterioration. According to FHWA and FTA (2014), before the enactment of MAP-21, approximately 83 % of bridges are inspected once every 24 months, 12% are inspected on a 12-month cycle due to advanced deterioration or other conditions warranting close monitoring, 5% of certain types of structures in satisfactory or better condition are inspected on a maximum 48-month cycle. However, biennial inspection frequency is still higher compared to the current practice in Japan where inspections take place every 5 years (MLTI 2014), and in other European countries such as France, Germany, Sweden, and Norway, which typically conduct detailed inspections every 6 years (Everett *et al.* 2008). Even within the previously stated countries, visual inspections are conducted on an annual basis or every 2 to 3 years. According to the AASHTO manual (AASHTO 2013), which is intended to be referred by FHWA (FHWA 2013), delamination is included as one of the bridge defects, which cannot be detected through visual inspection; thus, not only visual inspection, but also a hands-on inspection such as hammer sounding and chain drag to detect interior defects are needed biennially. Therefore, innovative technologies and processes that enable bridge administrators to inspect and evaluate bridge conditions more effectively and efficiently with less human and monetary resources are desired, especially in the United States.

1.2 Literature review

Traditionally, hammer sounding and/or chain dragging, and visual inspections have been implemented with qualified engineers and inspectors for concrete bridge deck evaluations. These methods, however, require a lot of field labor and lane closures, especially for bridge deck inspection. Instead of sounding tests, alternative Non-Destructive Evaluation (NDE) techniques such as Infrared Thermography (IRT), Ground-Penetrating Radar (GPR), and Impact Echo (IE) have been developed to detect subsurface delaminations, and computer vision-based damage detection methods have been utilized to detect surface defects as an alternative of visual inspection for efficient and effective bridge inspection. As well as the traditional inspection combination of visual and sounding inspections, no single method can detect all kinds of defects in concrete structures. The combination of IRT and computer vision-based techniques has the potential to replace/reduce the traditional methods of bridge inspection more efficiently and effectively since both techniques allow for non-contact application; hence, they can collect data from a moving platform. Especially in the case of bridge deck inspection, they can collect data at normal driving speeds and without any lane closures that are mostly required by traditional methods and other

NDE techniques. In fact, the combination of IRT and high-definition digital image system has been applied at normal driving speed for several years sometimes, although the ASTM standard suggests that no greater than 16 km/h (10 mph) for data collection speed of IRT (ASTM 2014).

In terms of visual inspection, the application of computer vision-based damage detection for concrete infrastructure has been exponentially increasing over the last decade, and automation of detection and measurements of defects has been developing (Koch *et al.* 2015). Especially for concrete bridge deck inspection, a Line Camera System (LCS) has been applied by attaching it to a vehicle that drives at normal speeds without any lane closures (Matsumoto *et al.* 2015, Wu *et al.* 2014). Regarding IRT, Gucunski *et al.* (2013), Vaghefi *et al.* (2013), Kee *et al.* (2012) and Oh *et al.* (2013) compared and evaluated each NDE technology for bridge deck deterioration detection at bridges in service. Vaghefi *et al.* (2013) compared IRT and chain drag at the locations of 10 core samplings; in this case, IRT showed 40% while chain drag performed 80% of accuracy for damage detection. On the other hand, in another comparative study at another bridge, one of IEs and IRT performed 100% accurate delamination detection at the locations of 8 core samplings, while chain dragging showed 75% accuracy (Oh *et al.* 2013). Gucunski *et al.* (2013) mentioned that IRT has a good potential for subsurface damage detection, although it was not the most accurate option among other NDE techniques.

Although there is a good amount of research on IRT up to the present, each study was conducted under different conditions, making it difficult to draw generalized conclusions. Therefore, there are still several uncertainties regarding the accuracy and reliability of IRT for application to bridge inspection when compared to sounding test (Catbas *et al.* 2015). Through literature reviews, it can be assumed that the following several factors might affect the performance of IRT

- 1) Data Collection Time: There are contradictory reports regarding appropriate time frames for IRT measurements. Washer *et al.* (2009) recommended daytime measurements 5 to 9 hours after sunrise to detect subsurface delamination; 5 to 7 hours after sunrise for 51 mm (2 in.) deep delamination, and 7 to 8 hours after sunrise for 76 mm (3 in.), for solar loading part. They also recommended 5 hours and 40 minutes after sunrise for 25-mm deep targets and more than 9 hours after sunrise for a target at a depth of 127 mm (4 in.) (Washer *et al.* 2010). On the other hand, others mentioned contrary conclusions; Gucunski *et al.* (2013) mentioned a thermal image recorded 40 minutes after sunrise yielded a much clearer image than another recorded around noon. Additionally, the response of delaminations were described as weaker in infrared (IR) images as the time approached 3 PM (Yehia *et al.* 2007). Moreover, Kee *et al.* (2012) also concluded that no indication was found from the IR image taken 3 hours and 45 minutes after sunrise (with the shallowest delamination located at 6.35 cm depth) while the best results were achieved using the cooling cycle in which even 15.24 cm deep delaminations could be detected. Furthermore, Watase *et al.* (2015) proposed favorable time for inspection depending on the parts of bridge; noon time for the deck top, and midnight for the deck soffit. Therefore, generalized ideal time for IRT data collection is not defined yet.
- 2) Size of Delamination: Some researchers indicated that the size of a delamination affects the detectable depth of the delamination (Abdel-qader *et al.* 2008, Cheng *et al.* 2008, Maierhofer *et al.* 2005, Yehia *et al.* 2007). However, each researcher has utilized artificial defects of different sizes and concluded different detectable depths for IRT; the effect of delamination size has not yet been clarified.

- 3) IR Camera Specifications: Since several types of hardware for other NDE methods such as IE and GPR have been compared, the comparative study showed different results depending on the device (Oh *et al.* 2013), IRT might also provide different results depending on the type of IR camera. In fact, some researchers have presented the effect of different camera specifications. Hashimoto and Akashi (2010) reported that IR cameras with more than 8 μm spectral range were affected by the reflection of the sky, and the effect is getting larger when the angle between IR camera and concrete surface becomes shallower, especially when the surface is smoother. They also took IR images of a bridge substructure using three types of cameras, Indium Antimonide (InSb) detector (1.5 – 5.1 μm), Quantum Well Infrared Photodetector (QWIP) detector (8 - 9 μm), and μ -bolometer detector (8 - 14 μm), with 45 degree of angle from the ground, and IR cameras equipped QWIP and μ -bolometer detectors captured reflected temperature of the sky. Nishikawa *et al.* (2000) also mentioned that the short wavelength (SW) machine is influenced by the reflection of the sun and the contrast of the sunshine and the shade, while the long wavelength (LW) machine is influenced by objects such as the sky and the opposite building. Thus, SW machines tend to be applied during nighttime, and LW machines tend to be used during daytime (Nakamura *et al.* 2013). In addition to spectral range, several other specifications can also be assumed that affect IRT performance such as integration time/time constant, detector type, pixel resolution, and thermal sensitivity.
- 4) Data Collection Speed: Although IRT has been applied for high-speed bridge deck scanning for several years sometimes, the ASTM standard recommends that less than 16 km/h (10 mph) for data collection speed (ASTM 2014). Therefore, when IRT is utilized while driving at normal speeds, there is a possibility that data collection speed also affects the result as it was mentioned by Hiasa *et al.* (2014) since the research on high speed application of IRT for bridge deck inspection has not been sufficiently implemented.

2. Research objectives

This study intends to explore factors which affect IRT for subsurface damage detection in concrete structures especially when IRT is utilized for bridge deck inspection while driving. Since most of bridge decks in the USA are made of concrete (93% - 343 km² out of 369 km² in bridge deck area by FHWA 2015), and concrete bridge decks deteriorate faster than other bridge components due to direct exposure to traffic (Gucunski *et al.* 2015), this study focuses on concrete bridge deck inspections by IRT. Particularly, the following are investigated in this study: a) IR cameras with different specifications, b) Photography conditions such as data collection times, driving speeds, camera angles while capturing images, c) Test specimens with different delaminations, d) Temperature condition, and e) Data analysis approaches.

As Gucunski *et al.* (2015) mentions, one of the limitations of NDE methods for bridge inspection is the speed of data collection. On the other hand, the valuable advantage of IRT is potential application for high-speed data collection; namely, the ability to inspect a bridge deck while driving at normal speeds without any lane closures in place of traditional sounding inspection or other NDE techniques which mostly require lane closures. This advantage can reduce dangers for both inspectors and motorists drastically since there are several potential dangers to closing a lane for inspection while cars are driving in the adjacent lanes. Furthermore, it can also

inspect much faster than other NDE methods. Since many experiments have been conducted with one IR camera, 3 different infrared cameras equipped with different specifications were utilized at the same time for a comparison of camera specifications. Furthermore, usual experiments on IRT have been conducted only under static conditions, so this study took IR images from a stopped and moving vehicle to investigate the effect of data collection speed. There are two types of applications for IRT, passive and active IRT. This study used passive IRT since it assumed the application of IRT for real bridges under natural circumstances. IR data was collected several times in a day to examine the effect of data collection time. In terms of size of delamination, only one delamination size was installed into test specimens. However, delaminations were set up at various depths from the surface.

In order to enhance reliability and applicability of IRT, especially for high-speed inspection of bridge decks, it is important to better understand the critical factors that degrade the performance of IRT. Thus, this study investigated several factors that might affect the performance of IRT, especially when IRT is utilized for high-speed bridge deck scanning.

3. Methods of the experiment

3.1 Infrared cameras

In this study, three infrared cameras with different specifications as shown in Table 1 (T420, T650sc and SC5600 manufactured by FLIR Systems, Inc.) were utilized to evaluate the differences of camera specifications and to avoid misconceptions by using only one IR camera test result. As mentioned above, since several types of hardware for IE and GPR were compared and produced different results, IRT must also be compared with different types of IR hardware to accurately evaluate the difference in inspection reliability.

Table 1 Three infrared cameras used in this study and their primary specifications

Camera Type	T420	T650sc	SC5600
Detector Type	Uncooled microbolometer	Uncooled microbolometer	InSb
Thermal sensitivity (NETD)	< 0.045° at 30°C	< 0.02°C at 30°C	< 0.02°C at 25°C
Accuracy	±2°C or ±2%	±1°C or ±1%	±1°C or ±1%
Resolution	320 × 240 pixels	640 × 480 pixels	640 × 512 pixels
Spectral range	7.5 – 13 μm	7.5 – 14 μm	2.5 – 5.1 μm
Frame Rate	60 Hz	30 Hz	100 Hz
Field of View	25°×19°	25°×19°	20°×15°
Integration Time/ Time Constant (Electronic Shutter Speed)	12 ms	8 ms	10 μs to 20 ms

As shown in Table 1, T420 and T650sc have the same type of detector, uncooled micro bolometer, while SC5600 has an InSb detector. IR cameras can be classified into two types according to their detector type: thermal detectors and quantum detectors. These are often called uncooled and cooled detectors/cameras respectively. Since the effect of camera specifications has not been discussed very much so far, many researchers used uncooled cameras which have similar specifications to T420 and T650sc due to economic reasons. Typically, uncooled cameras have lower costs and a broader spectral response than cooled cameras, although their response is much slower and less sensitive than cooled cameras (FLIR 2013). In terms of the IR cameras used in this study, SC5600 captures medium wavelength while others capture long wavelength. Furthermore, SC5600 has much shorter integration time (time constant for uncooled cameras) than others, and it helps to capture the exact figure of objects under high speed application without image blur (FLIR 2015). Regarding the other aspects with the exception of detector type, SC5600 and T650sc have approximately the same imaging resolution, and T420 has lower resolution. Moreover, SC5600 and T650sc have the same thermal sensitivity, and it is two times more sensitive than T420. Therefore, the differences in detector type, spectral range, integration time (time constant), thermal sensitivity, and resolution are comparable. The results obtained by three different IR cameras were compared to show how the specifications of each have evident effects on the degree of accuracy in the detection of subsurface delaminations within concrete structures.

3.2 Test specimens

In this study, four concrete test specimens were made for this experiment to compare the performance of three different IR cameras. These specimens have artificial delaminations, each size is 10.2 cm (4 in.) \times 10.2 cm \times approximately 3.18 mm (1/8 in.), made by foamed sheet and cardboard wrapped in plastic as shown in Fig. 1 at a different depth from the concrete surface, 1.27 cm (0.5 in.), 2.54 cm (1 in.), 5.08 cm (2 in.) and 7.62 cm (3 in.). The depth of the deepest delamination was decided based on literature noting detection of delamination at up to 7.62 cm deep from the surface for 20.3 cm (8 in.) thickness of concrete specimens (Abdel-qader *et al.* 2008). Each concrete test specimen made for this experiment was designed as the same thickness, and the size is 91.4 cm (3 ft.) \times 91.4 cm \times 20.3 cm as described in Fig. 1. The slab thickness was designed to simulate a typical bridge deck in the USA. Although the past experiment was conducted in an active thermography manner and was carried out inside a lab (Abdel-qader *et al.* 2008), the same depth was repeated in this study to observe the effects of the natural environment. In terms of the depth of 5.08 cm, it was chosen to investigate the detectability of defects around reinforcing bars by IRT, since the top concrete cover for a bridge deck is typically 5.08 cm (2 in.), and many delaminations occurred around them for concrete structures due to corrosion of the reinforcing steel (Washer *et al.* 2010). Other shallower delaminations were located at half of it, 2.54 cm, and the half depth of 2.54 cm, 1.27 cm for the comparison. Since this experiment aims to detect artificial anomalies which reproduces inner cracks/voids, reinforcing bars were not installed in these concrete slabs.

Foamed sheet was installed at the center part of the specimen and wrapped cardboard was embedded at a corner as shown in Fig. 1. The thermal conductivity of air, which exists at the delaminated area of concrete and creates the temperature difference between sound and delaminated parts of concrete surface, is 0.0241 W/m \cdot °C. Foamed sheet and cardboard were chosen to generate the artificial delamination to simulate similar thermal conductivity properties.

The thermal conductivity of the foamed sheet is $0.024 \text{ W/m}\cdot^{\circ}\text{C}$, and the cardboard has a lot of airspace on the inward side.

3.3 Photography conditions

Fig. 2 shows the test location, Ara Drive, in front of the Stormwater Research Lab at the University of Central Florida. The field test was conducted on January 21, 2015. As shown in Fig. 2, 4 concrete test specimens were set up along the roadside. In this experiment, concrete blocks were put on wooden stands and pallets to make space through which wind blows under concrete slabs as shown in the picture. IR images were taken from a vehicle equipped with the three IR cameras at the same time while driving down the road at varying speed, from 0 to 48 km/h (30 mph). 0 km/h refers to an idling stop, so that the engine was working during the photography. Therefore, there was some vibration of the car due to idling even when the speed was 0 km/h. IR images were taken at multiple times, 9 am, 3 pm, 8 pm and 12 am.

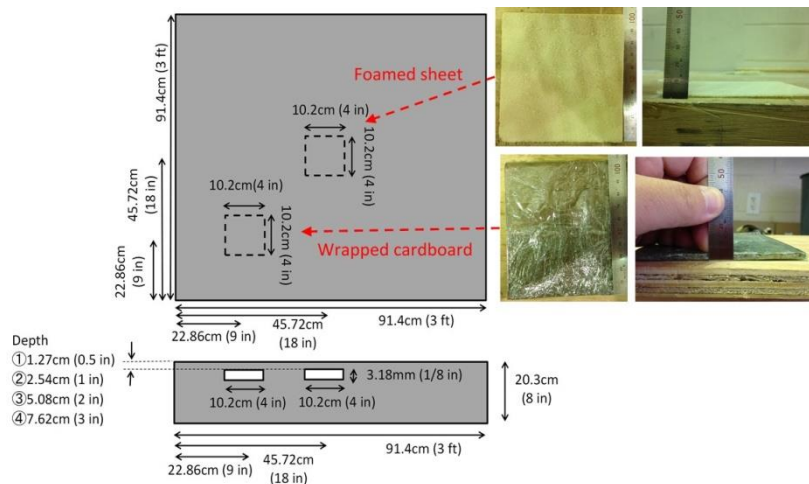


Fig. 1 Size of concrete test specimen



Fig. 2 Test location and method

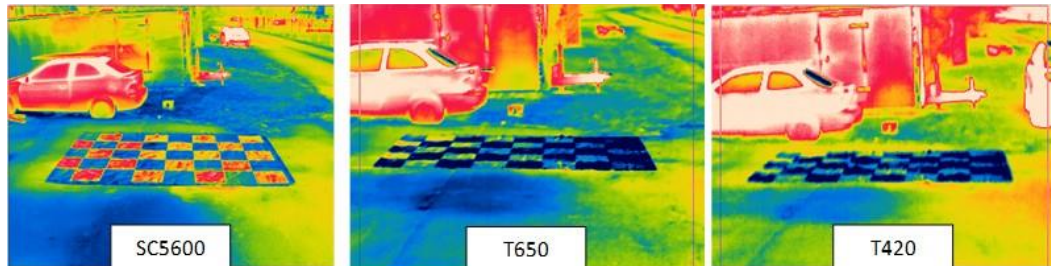


Fig. 3 Camera position

Each camera's position was set up with an angle between 45° to 50° (where 0° is perpendicular) to capture the same width at the center of the image. As shown in Fig. 3, each camera's position was calibrated with the help of a plastic calibration sheet (3.5×2.42 m). The width was assumed to capture one lane of roadway width at one time. Due to the different Field of View for each IR camera, their images look different when comparing SC5600 with the other two cameras.

3.4 Data analyzing methodology

Theoretically, delaminated areas show a hot spot during daylight and a cool spot at nighttime. However, it is not always possible to detect subsurface delaminations in concrete structures only from the color variation of raw infrared imagery since the concrete structure itself tends to have a temperature gradient depending on location and orientation with respect to the sun as discussed by Washer *et al.* (2010). Since specific processes are desirable to obtain a better result from IRT as mentioned in (Kee *et al.* 2012, Oh *et al.* 2013), an infrared image processing software (Matsumoto *et al.* 2012) was utilized in this study. This software indicates potential delaminated areas which have cooler (hotter) temperature distribution than the surroundings during nighttime (daytime) with three categories, red, yellow and green colors in the order of severity, classified depending on magnitude of the temperature contrast. In this software, the higher contrast area is evaluated as a more severe delamination. Fig. 4 shows the methodology of analysis in this study. Since IR cameras were mounted on top of the vehicle and images of test specimens on the roadside were taken at a certain angle, the original IR images become like the upper images of (a) with rainbow color. In the original IR images, since the concrete blocks were located at the left side of the image with a certain angle, it was difficult to compare each specimen and figure. Furthermore, as shown in the lower images, even images processed by the software produce a lot of noise because the specimens were placed on a grass field. Therefore, these images were deskewed into plain view to make it much easier to compare with others by compensating the original image. Since the size of the specimens were known, the surface is $91.4 \text{ cm} \times 91.4 \text{ cm}$, each image of a test specimen was compensated into plain view, and other parts were trimmed except for the surface of concrete test specimens as shown in the (b) of Fig. 4.

3.5 Temperature

Through the experiment, ambient temperature and surface temperature of test specimens were recorded by thermocouples. For the test specimens, thermocouples were attached onto them with

artificial delaminations at 1.27 cm and 7.62 cm depth. One thermocouple was attached on the sound concrete surface, and another one measured ambient temperature for each test specimen as shown in the right two images of Fig. 5. Furthermore, in order to monitor the ambient temperature of the test field, one thermocouple was attached on a shed wall in the shade for the day's entirety near the test site as shown in left image of Fig. 5. The temperature record is shown in Fig. 6. In this graph, the records of thermocouples attached on a concrete slab with 1.27 cm deep delamination are described as "con 1.27", which attached on the surface, and "con 1.27 air", which set up a shaded part made by the specimen to measure air temperature near the concrete slab. The legends of thermocouples attached on a concrete slab with 7.62 cm deep delamination are similarly provided. The "air" shows the temperature that measured ambient temperature of the test field at the shed. In terms of ambient temperature, the temperature difference between the highest and lowest air temperature in a day (from 8 am to 1 am in this study) was approximately 12°C by "air" (max: 23.7°C, min: 11.6°C), and approximately 16°C near concrete slabs ("con 1.27 air": 26.9 and 10.8°C, "con 7.62 air": 26.6 and 10.6°C). Regarding surface temperatures, thermocouples seem to be affected by sunlight since those temperatures are unstable in the daytime and sometimes they decreased drastically. It can be considered that clouds and trees around the test field made shadows sometimes, and they caused temperature variations in the daytime.

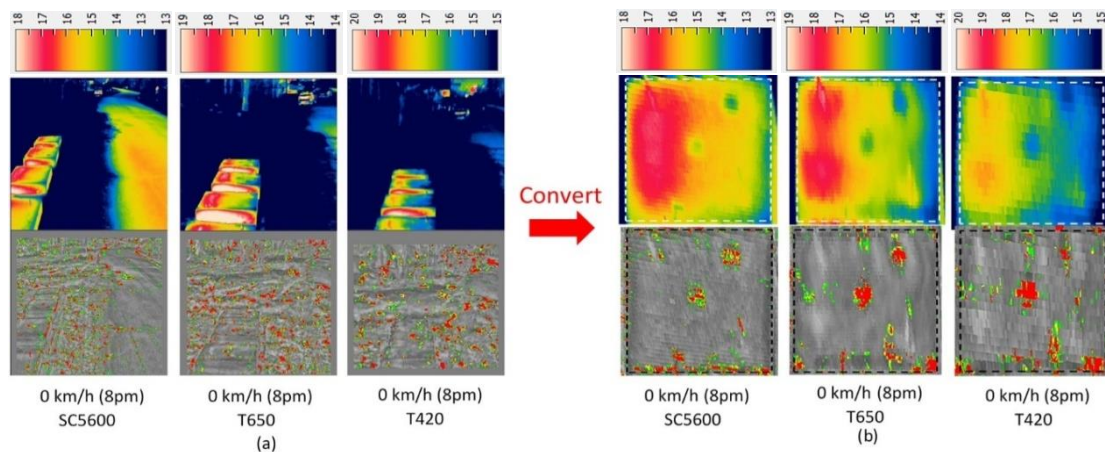


Fig. 4 Original IR and processed images (a) and converted images and (b) at 8 PM (Temperature: °C)



Fig. 5 Temperature measurement

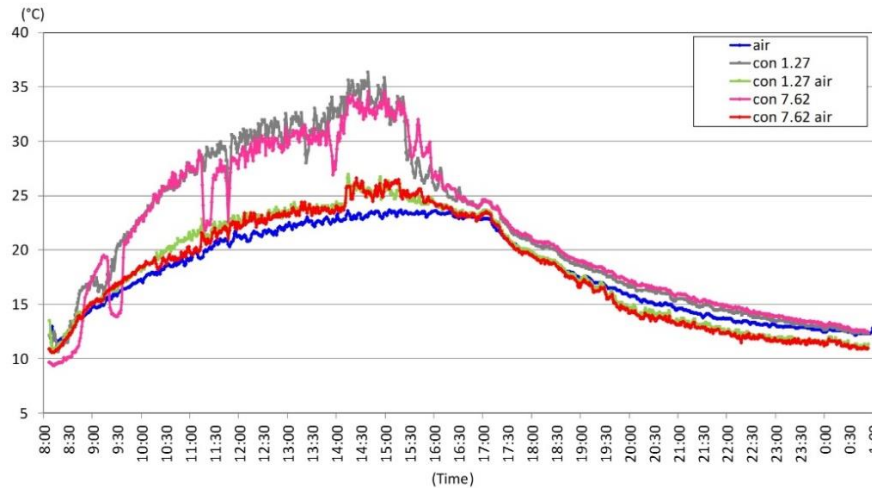


Fig. 6 Temperature during test

4. Test results

4.1 Results of damage detection by both raw IR and processed images

Fig. 7 shows raw IR and processed images of the concrete slab with 1.27 cm depth of delamination taken at 9 am, 3 pm, 8 pm and 12 am at 0 km/h and 48 km/h. The temperature range of the IR images is set up to 5 K for all images except images at 3 pm (10 K) since the temperature distribution at 3 pm is much wider than at other times. Two types of delamination described in Fig. 1 were embedded at the center and the corner of the block (upper right side for 1.27cm depth). In this study, both raw IR and processed images were investigated to determine whether those images could detect delaminated spots or not.

Table 2 summarizes the results. Delaminations detected clearly are listed as a circle symbol, an obscure defect is marked as a triangle symbol, and non-detected delaminations are marked as x-marks. If there are any differences between SC5600 and the other two cameras, those parts are described by a boldface mark in the table. In this study, when the concrete blocks were casted, carrying handles were set up at the two corners on a diagonal line to a reversed position of the cardboard delamination by reinforcing bars (upper left and lower right corners of the images in Fig. 7). Furthermore, thermocouple was attached on the surface, lower end of the images in Fig. 7. Since they have a different temperature distribution from the concrete surface, they were not considered as delaminations even though IR and processed images indicated them as delaminated parts. Moreover, since the temperature of the concrete surface was not entirely homogeneous temperature distribution due to boundary conditions and the effect of sunlight, and so on, some temperature differences were judged as noise or errors, namely, they were evaluated as sound areas. This method becomes relatively subjective because the locations of the delaminated parts were known beforehand.

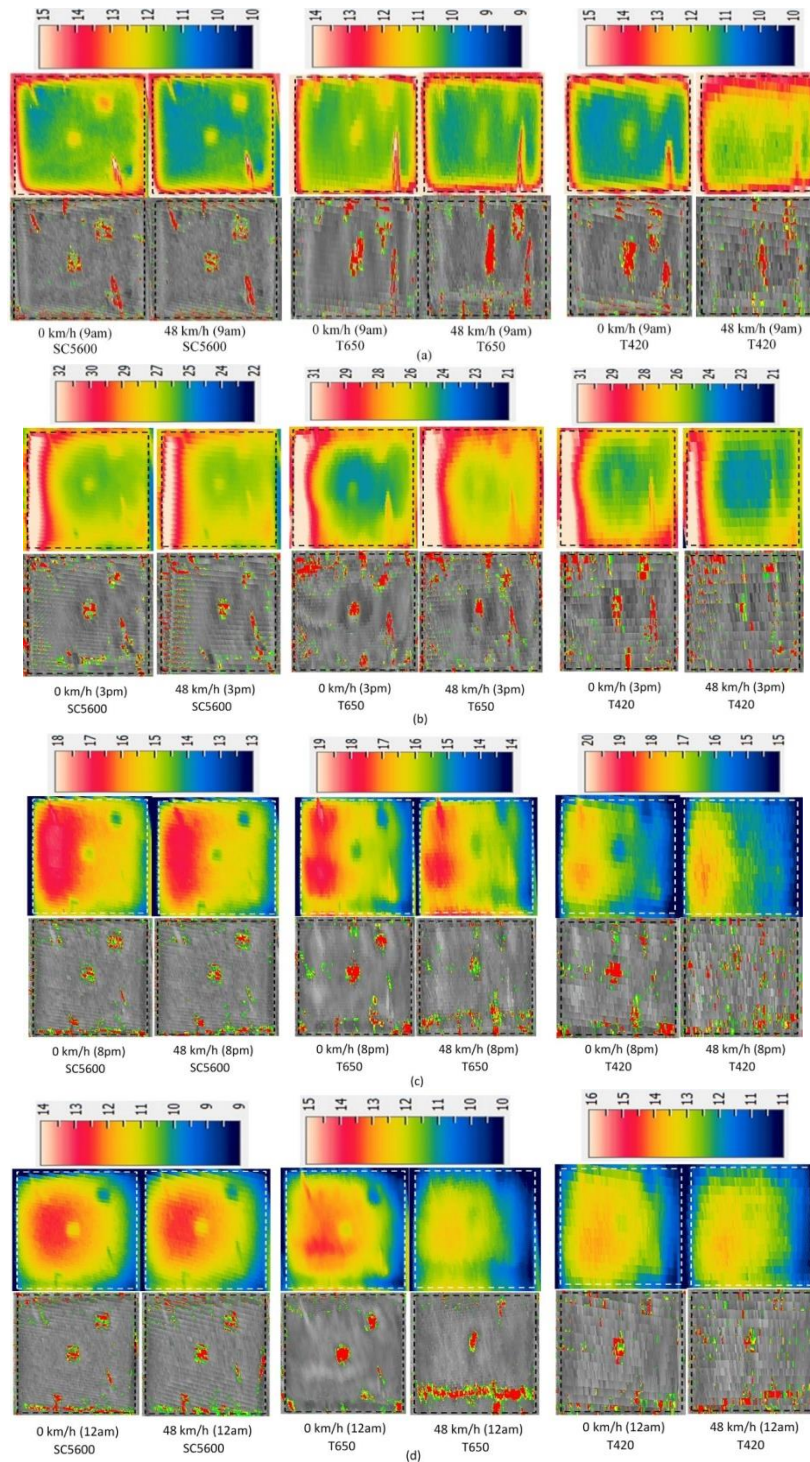


Fig. 7 Comparison of 1.27 cm (0.5 in.) depth images taken at 0 km/h (left) & 48 km/h (right): (a) 9 am, (b) 3 pm, (c) 8 pm and (d) 12 am (Temperature: °C)

Table 2 Result of delamination detection

Time	Depth (cm)	SC5600								T650sc								T420							
		0 km/h				48 km/h				0 km/h				48 km/h				0 km/h				48 km/h			
		Raw IR	Processed IR	Raw IR	Processed IR	Raw IR	Processed IR	Raw IR	Processed IR	Raw IR	Processed IR	Raw IR	Processed IR	Raw IR	Processed IR	Raw IR	Processed IR	Raw IR	Processed IR	Raw IR	Processed IR				
		middle	corner	middle	corner	middle	corner	middle	corner	middle	corner	middle	corner	middle	corner	middle	corner	middle	corner	middle	corner	middle	corner	middle	corner
9AM	1.27	○	○	○	○	○	○	○	○	○	○	○	○	△	△	○	○	○	○	○	○	○	○	○	○
	2.54	○	○	○	○	○	○	○	○	○	○	○	○	△	△	○	○	○	△	○	○	○	○	○	○
	5.08	X	X	X	X	X	X	X	X	X	X	X	X	X	X	X	X	X	X	X	X	X	X	X	X
	7.62	X	X	X	X	X	X	X	X	X	X	X	X	X	X	X	X	X	X	X	X	X	X	X	X
3PM	1.27	○	○	○	○	○	○	○	○	○	○	○	○	X	X	○	○	○	△	○	○	X	X	△	△
	2.54	○	○	○	○	○	○	○	○	○	○	○	○	△	△	○	○	○	○	○	○	○	○	○	○
	5.08	X	X	X	X	X	X	X	X	X	X	X	X	X	X	X	X	X	X	X	X	X	X	X	X
	7.62	X	X	X	X	X	X	X	X	X	X	X	X	X	X	X	X	X	X	X	X	X	X	X	X
8PM	1.27	○	○	○	○	○	○	○	○	○	○	○	○	△	△	○	○	○	○	○	○	△	△	△	△
	2.54	○	○	○	○	○	○	○	○	○	○	○	○	△	△	○	○	○	○	○	○	△	△	○	○
	5.08	X	X	△	△	X	X	△	△	X	X	△	△	X	X	X	X	X	X	X	X	X	X	X	X
	7.62	X	X	X	X	X	X	X	X	X	X	X	X	X	X	X	X	X	X	X	X	X	X	X	X
12AM	1.27	○	○	○	○	○	○	○	○	○	○	○	○	△	△	○	○	△	△	△	△	X	X	△	△
	2.54	○	○	○	○	○	○	○	○	○	○	○	○	△	△	○	○	△	△	△	△	X	X	△	△
	5.08	X	X	X	X	X	X	X	X	X	X	X	X	△	△	X	X	△	△	△	△	X	X	X	X
	7.62	X	X	X	X	X	X	X	X	X	X	X	X	△	△	X	X	△	△	△	△	X	X	X	X

○: Detected the delamination clearly
 △: Detected the delamination, but the indication is obscure
 X: Not detected the delamination

4.2 Effect of camera specifications for IRT performance

As can be seen, the SC5600 showed the highest performance at any time and any speed. Then, T650sc performed better than T420. In terms of the effect of data collection speed, when T650sc and T420 took IR images at 48 km/h, indications of delamination became more unclear and larger than those taken at 0 km/h. The reason can be due to the much slower integration time (time constant) of uncooled cameras than that of cooled cameras, and that made blurred images, since SC5600 did not show any differences between images taken at 0 km/h and 48 km/h at any time. Also, T650sc and T420 show relatively larger indication compared to SC5600 even with images taken at 0 km/h. This shows that even the vibration caused by the idling of the car affects the result of IRT with IR cameras which have longer integration time (time constant).

Regarding the effect of pixel resolution, images of T420 are much rougher than images of the other two cameras as can be seen in Fig. 7, and that makes it difficult to detect delaminations. Since T420 has 4 times lower resolution than the other two cameras, each pixel of T420 image can be distinguished easily from Fig. 7, and the larger pixels make T420 more insensitive than the other two cameras. In this study, three cameras set up to take one whole lane of a roadway as mentioned in section 3.3, so that the distance to the concrete slabs might be out of the coverage for T420. The approximate size of each pixel is as follows; SC5600 and T650sc: 0.5 cm × 2.0 cm, T420: 1.0 cm × 4.0 cm, although each pixel size is not always the same since IR images were taken with a certain angle. The upper side of the image was rougher than the underside of the image, and they were not taken at the exact same locations. It can be concluded that the main factor for lower performance of T420 than T650sc was the lower pixel resolution. When the camera angle of T420 was changed to make the distance between the camera and concrete slabs, the images became much clearer as shown in the left image of Fig. 8. In this image, each pixel size is approximately 0.3 cm × 0.7 cm. However, even though the image quality was improved drastically by taking a closer distance, the area that can be taken at one time became much smaller, here it was about 1 m width. Therefore, if T420 is used for bridge deck inspection and it is

required to provide the same quality as T650sc, data collection must be implemented three or four times more than T650sc, or three or four cameras should be used at the same time to collect data of whole one lane, about 3.6 m width typically. Furthermore, when T420 was used to take a closer distance at driving speed, those images were more blurred as shown in the right image of Fig. 8. This can be due to the much longer time constant of uncooled IR cameras. These results indicate that 640×480 pixels for pixel resolution is preferable for efficient bridge deck inspection, and only static photography is recommended for uncooled cameras.

In terms of other specifications such as spectral range and thermal sensitivity, those effects could not be clarified by these comparisons.

4.3 Effect of data collection speed for IRT performance

In order to evaluate how much data collection speed affected IRT performance for damage detection, the results showed in Table 2 are evaluated by numerical scoring as follows: circles are 1.0, triangles are 0.5, and x-marks are 0.0. Since 5.08 and 7.62 cm deep delaminations were not detected in this experiment, up to 2.54 cm depth of delaminations were evaluated, so that the score is counted by the four delaminations of 1.27 and 2.54 cm deep at the center and corner for each time and speed. Therefore, the maximum score is 4 for each time and speed. The scaling result is summarized as shown in Table 3. Even though the score of SC5600 at each time and speed is never changed for both “Raw IR” and “Processed IR”, both scores of T650sc and T420 are degraded when they are used at 48 km/h, especially for “Raw IR”. Since SC5600 and T650sc performed almost similar levels of damage detection at 0 km/h and only T650sc showed lower performance at 48 km/h, the main factor that affects high-speed application of IRT is the longer time constant (integration time) of uncooled IR cameras. Regarding the lower performance of T420, the reason can be due to the lower resolution of the camera as mentioned in section 4.2.

This comparison also found that processed images are very useful to detect delaminated parts when IR data are collected from moving vehicles. Especially for uncooled cameras, the performance of damage detection for high-speed inspection improved drastically: about 80% for T650sc and 150% for T420. Therefore, it can be concluded that when IRT with uncooled cameras are utilized for high-speed inspection, the IR image is affected by the speed of the data collection. However, relatively reliable data can be obtained by processing the images, although the performance is worse than cooled cameras.

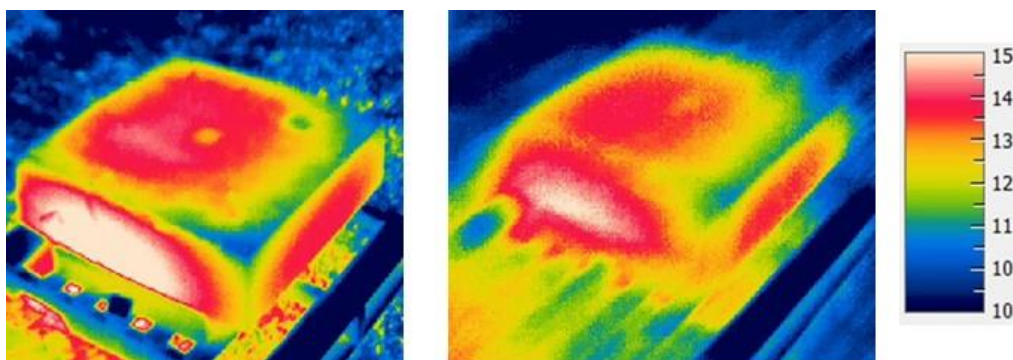


Fig. 8 IR image taken by T420 with different angle and closer distance (left: 0 km/h, right: 48 km/h, 12 am, 1.27 cm, Temperature: °C)

Moreover, areas of each indicated delamination spot for 1.27 and 2.54 cm deep were measured manually, and the percentage of indicated area to the concrete surface is summarized in Table 4. In this study, each delaminated spot area is designed to be approximate 1.25% of concrete slab surface area; area of delamination is 10.2 cm \times 10.2 cm and area of slab surface is 91.4 cm \times 91.4 cm. Although this comparison is relatively subjective since the locations of delamination are known, the average ratios of SC5600 are very close to the designed ratio regardless of data collection speed for raw and processed IR images, and their average and standard deviation are not changed even when the speed is 48 km/h. Regarding T650sc, the average ratios are larger than designed, one even 0 km/h, and they are getting larger when it is used at 48 km/h. Furthermore, the standard deviations at 48 km/h become much larger than at 0 km/h. The main differences between SC5600 and T650sc are integration time, which mostly depends on whether cooled or uncooled detector type, or spectral range, which is either SW or LW. In this comparison, since only T650sc was affected by data collection speed when it was used while driving, it can be concluded that the main factor which affects high-speed application is much longer integration time. It can be assumed that the reason why T650sc shows relatively larger indications than real size is that it was affected by the vibration of idling even at 0 km/h as mentioned above. As for T420, it failed to detect delaminations when it was used at 48 km/h in many cases from raw IR data, so that it is difficult to compare raw IR data, yet averages and standard deviations in any case for T420 are much larger than the other two cameras. The reason is that there was not only a much longer time constant, but also lower pixel resolution.

Furthermore, Fig. 9 to Fig. 11 show histograms of the ratios of indicated area to the slab surface at 0 km/h and 48 km/h regardless of raw or processed IR images. From Fig. 9, it is obvious that almost every result of SC5600 distributes between a 1 to 2 percent range of both 0 km/h and 48 km/h. This result proves that SC5600 detects very accurately even when it is utilized on a moving vehicle at normal driving speed. As for T650sc, the range became wider, from 1 to 2.5%, at 0 km/h, and when it was used at 48 km/h, the distribution became wider than those taken at 0 km/h and in some cases it failed to detect delaminations as shown in Fig. 10. T420 degraded more than T650sc when it was used at 48 km/h as described in Fig. 11. Therefore, this study concludes that these two cameras are strongly affected by data collection speed, and the main factor is their much longer time constant than cooled IR cameras.

Table 3 Scaling of delamination detection for each time and speed

1.27, 2.54 cm		SC5600			T650sc			T420		
		0 km/h	48 km/h	Degradation	0 km/h	48 km/h	Degradation	0 km/h	48 km/h	Degradation
Raw IR	9am	4.0	4.0	N/A	4.0	2.5	-38%	3.5	0.0	-100%
	3pm	4.0	4.0	N/A	4.0	0.5	-88%	3.5	2.0	-43%
	8pm	4.0	4.0	N/A	4.0	3.5	-13%	4.0	2.0	-50%
	12am	4.0	4.0	N/A	3.5	2.0	-43%	2.0	0.0	-100%
Processed IR	9am	4.0	4.0	N/A	4.0	4.0	N/A	4.0	4.0	N/A
	3pm	4.0	4.0	N/A	4.0	4.0	N/A	4.0	3.0	-25%
	8pm	4.0	4.0	N/A	4.0	3.5	-13%	3.5	2.5	-29%
	12am	4.0	4.0	N/A	4.0	4.0	N/A	2.0	0.5	-75%
Raw IR total		16.0	16.0	N/A	15.5	8.5	-45%	13.0	4.0	-69%
Processed IR total		16.0	16.0	N/A	16.0	15.5	-3%	13.5	10.0	-26%
Improvement		N/A	N/A		3%	82%		4%	150%	

Table 4 Comparison of the percentage of indicated area to the concrete surface area

TIME	DEPTH (cm)	Defect location	SC5600				T650sc				T420			
			Raw IR		Processed IR		Raw IR		Processed IR		Raw IR		Processed IR	
			0 (km/h)	48 (km/h)	0 (km/h)	48 (km/h)	0 (km/h)	48 (km/h)	0 (km/h)	48 (km/h)	0 (km/h)	48 (km/h)	0 (km/h)	48 (km/h)
9AM	1.27	middle	1.13%	1.75%	1.80%	1.72%	2.47%	5.99%	3.95%	4.88%	8.49%	-	4.88%	4.24%
			1.44%	1.52%	1.94%	1.66%	3.08%	4.47%	2.22%	3.86%	2.66%	-	2.85%	3.56%
	2.54	corner	2.00%	2.24%	2.86%	2.43%	2.74%	4.23%	2.83%	4.01%	3.41%	-	4.79%	3.66%
			1.80%	1.72%	2.12%	1.81%	1.84%	3.78%	2.54%	3.92%	2.74%	-	3.76%	3.59%
3PM	1.27	middle	1.07%	0.92%	1.50%	1.54%	1.72%	-	1.45%	1.15%	3.54%	-	2.89%	1.97%
			1.25%	1.57%	1.52%	1.73%	1.32%	-	2.15%	2.05%	1.52%	1.95%	1.59%	2.08%
	2.54	corner	1.80%	1.22%	1.10%	0.94%	2.39%	-	1.86%	2.97%	2.71%	-	2.38%	1.59%
			1.40%	1.47%	1.63%	1.53%	1.58%	-	1.72%	2.10%	2.54%	1.28%	2.44%	2.16%
8PM	1.27	middle	1.36%	0.91%	1.92%	1.52%	2.16%	3.15%	1.87%	1.96%	4.16%	-	2.43%	-
			0.63%	0.43%	1.67%	1.47%	1.53%	1.56%	1.65%	1.80%	1.55%	1.39%	1.51%	1.58%
	2.54	corner	1.46%	1.37%	1.53%	1.91%	2.33%	2.91%	1.46%	0.40%	2.87%	-	1.44%	-
			1.38%	1.23%	1.58%	1.54%	1.61%	1.72%	1.58%	1.26%	1.50%	2.77%	0.91%	1.46%
12AM	1.27	middle	1.45%	1.72%	1.65%	1.79%	1.33%	2.57%	1.95%	1.18%	1.67%	2.54%	2.59%	2.00%
			1.10%	1.20%	1.09%	1.25%	1.37%	1.15%	2.36%	1.19%	2.54%	-	1.35%	1.19%
	2.54	corner	1.49%	1.61%	1.57%	1.76%	2.08%	1.68%	1.02%	1.14%	2.56%	3.97%	1.56%	1.66%
			1.05%	1.14%	1.23%	1.15%	2.05%	2.35%	2.48%	1.23%	2.76%	-	1.98%	1.52%
Average			1.36%	1.38%	1.67%	1.61%	1.98%	2.96%	2.07%	2.19%	2.95%	2.32%	2.46%	2.31%
Standard Deviation			0.32%	0.41%	0.41%	0.33%	0.51%	1.38%	0.67%	1.28%	1.60%	0.92%	1.14%	0.97%

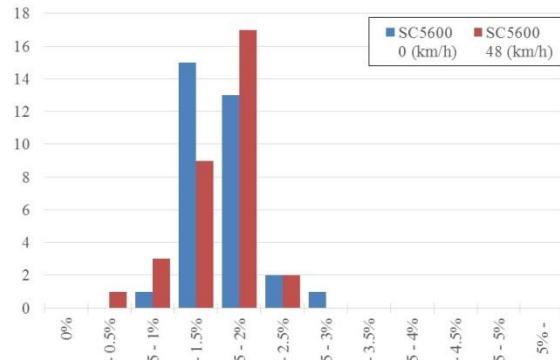


Fig. 9 Distribution of indicated damage area size ratio by SC5600

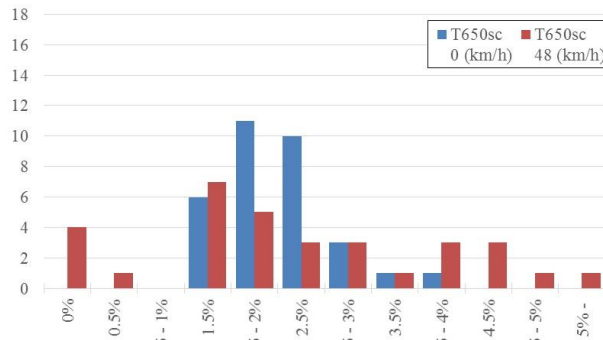


Fig. 10 Distribution of indicated damage area size ratio by T650sc

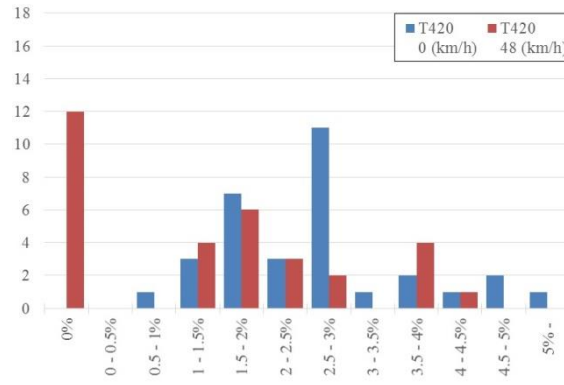


Fig. 11 Distribution of indicated damage area size ratio by T420

4.4 Detectable depth of delamination for IRT

In terms of detectable depth of the delamination in the concrete slabs, up to 2.54 cm (1 in.) depth can be detected clearly in any cases for SC5600. As for T650sc and T420, up to 2.54 cm depth can be detected at 0 km/h, even though some of them are not clear. However, when data were collected at 48 km/h, IR images become obscure or cannot detect delaminated areas especially from the raw IR images. Furthermore, since the locations of delaminated parts are known, the judgment tends to be subjective for T650sc and T420 even though those images are unclear and it would be challenging to distinguish in a blind test. Therefore, it can be assumed that detecting delaminations from real concrete structures by an uncooled camera becomes more difficult, especially when it is utilized for high-speed applications.

Furthermore, for 5.08 cm (2 in.) depth delamination, only SC5600 indicates the potential that can detect delamination up to 5.08 cm by processed images in any speed as shown in Fig. 12, although the shapes are not exactly square. In some research, however, IRT detected 5.08 cm or deeper delaminations; therefore, it can be considered that SC5600 might be able to detect delamination at 5.08 cm depth from the surface under the desirable environmental condition, or if larger size of delamination is used as assumed in section 1.2.

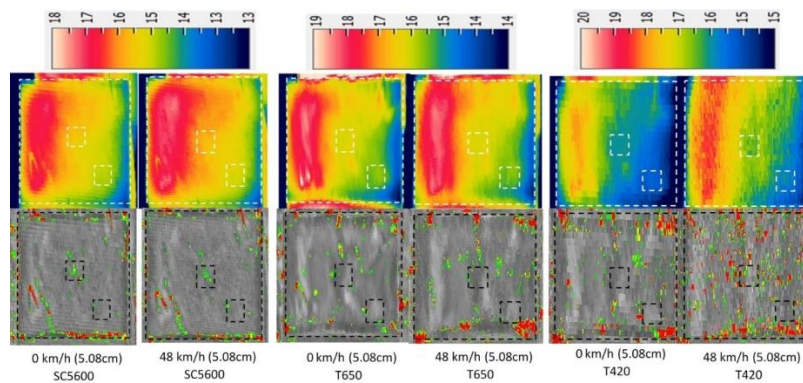


Fig. 12 Comparison of 5.08 cm depth images taken at 0 km/h and 48 km/h at 8 pm (Temperature: °C)

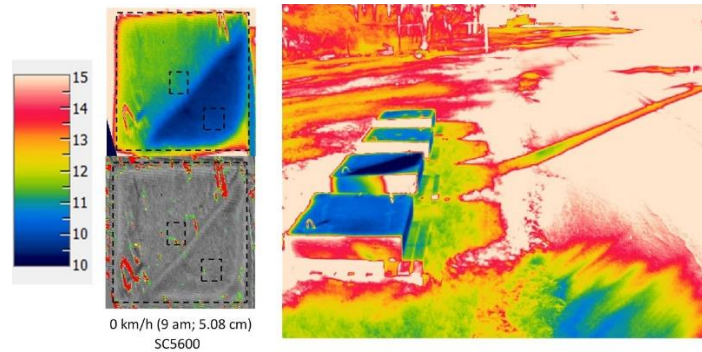


Fig. 13 Effect of sunlight: left; deskewed, right; original (9 am: SC5600; 0km/h)

4.5 Environmental effects for IRT

The images on the left of Fig. 13 show deskewed IR and processed images taken at 9 am at 0 km/h by SC5600 for the test piece has 5.08 cm deep delamination, and the image on the right is the original IR image. Both IR images clearly show a temperature difference between the upper left side and lower right side of the concrete surface. This difference was caused by the shadow of a tree which was located behind the test site. This result shows that if there is a shaded part on the concrete surface, the result of IRT is strongly affected by sunlight and shadow even in the morning. As a matter of fact, measured concrete surface temperatures of 1.27 and 7.62 cm depth delamination test specimens in Fig. 6 show drastic temperature changes sometimes from after sunrise until sunset respectively at different times even though they are located close to each other. It can be explained by the effect of shadows due to clouds or surrounding trees. Furthermore, the range of temperature change on the concrete surface during daytime, around 11 am to 5 pm, is much larger than the range during the morning or nighttime. As shown in Fig. 7(b), in spite of the temperature range of IR image at 3 pm being 2 times wider than at other times, the left edge part shows much higher temperature than the right part; actually, it exceeds the temperature range. It is also apparent that the concrete surface temperatures vary from one place to another. Therefore, it can be assumed that there is more “noise” during the daytime since the concrete surface temperature is randomly changing with a much wider range than morning or nighttime from time to time, and from one place to another as it is mentioned by Kee *et al.* (2012). Based on these results, it can be concluded that direct sunlight strongly affects the assessment results of IRT, and nighttime would be the suitable time window for IRT due to less false detections and interferences of sunlight, although further experiments are needed.

5. Conclusions

In this research, three IR cameras with different specifications were compared at different times and speeds of data collection to explore several factors which affect IRT for subsurface damage detection in concrete structures, especially when IRT is utilized for high-speed bridge deck inspection at normal driving speeds. Four concrete test specimens with artificial delaminations

were prepared for this experiment. The results show that IRT can detect up to 2.54 cm delamination from a concrete surface at any time period in this experiment. However, there should be an undetectable time zone when the delaminated and sound parts form an equilibrium state in the early morning and evening as it is assumed by Matsumoto *et al.* (2012). Since the delaminated area was already hotter than the surroundings at 9 am, the equilibrium state must be earlier than 9 am under the condition of this test. Similarly, that area was cooler than the surroundings at 8 pm, so that it must be earlier than 8 pm.

In terms of the effect of data collection speed, the main factor that affects high-speed application of IRT is the much longer time constant (integration time) of uncooled IR cameras since the cooled camera used for this study, SC5600, did not show any differences between images taken at 0 km/h and 48 km/h at any time. This study proved that SC5600 detected very accurately even when it was utilized with a moving vehicle at normal driving speed. On the other hand, uncooled cameras, T650sc and T420, were strongly affected by data collection speed, and when they were used at 48 km/h, their damage indication became larger than those taken at 0 km/h. Therefore, this study concludes that when IRT with uncooled cameras are utilized for high-speed inspection, the IR image is affected by the speed of the data collection.

Regarding the effect of pixel resolution, lower pixel resolution, 320×240 pixels, caused much lower performance when the camera was attached on a vehicle to take images of one lane width of a roadway, and this result indicates that 640×480 pixels for pixel resolution is preferable for efficient bridge deck inspection. Even though IR cameras with lower resolution can take better quality images due to the closer distance, the area that can be taken at one time also became much smaller. Thus, data collection must be implemented three or four times more than higher resolution cameras, or three or four cameras should be used at the same time to collect data of one lane completely.

It is also apparent that the concrete surface temperatures vary from one place to another during daytime. Therefore, it can be assumed that there is more “noise” during the daytime since the concrete surface temperature is randomly changing with a much wider range than morning or nighttime from time to time, and from one place to another. Based on these results, it can be concluded that direct sunlight strongly affects the assessment results of IRT, and nighttime would be the suitable time window for IRT due to less false detections and interferences of sunlight, although further experiments are needed.

In terms of other specifications such as spectral range and thermal sensitivity, those effects require further studies. Moreover, other types of cooled detectors such as QWIP, PtSi and MCT, which have different specifications and are not compared in this study, should also be compared. This study, however, was able to reveal two important factors of camera specifications for efficient bridge deck inspection by IRT. Shorter integration time, which cooled type cameras are typically equipped, enables high-speed inspection at normal driving speed without any lane closures while having the same level of accuracy and reliability as when IRT is used under a static situation. In addition, higher pixel resolution is also preferred to inspect larger areas of bridge decks at one time.

Acknowledgments

The research study presented in this paper is supported by West Nippon Expressway Company Limited. The authors are grateful for the opportunity and support for making this study possible.

We would like to express sincere appreciation to Mr. Juan Cruz and our other research group members for their support with manufacturing test specimens and setting up equipment. Particularly, we would like to thank Mr. Shinji Nagayasu, Mr. Kyle Ruske, (NEXCO-West USA) for their help and contribution to this project.

References

- AASHTO. (2013), Manual for Bridge Element Inspection, 1st Edition, with 2015 Interim Revisions.pdf.
- Abdel-qader, I., Yohali, S., Abudayyeh, O. and Yehia, S. (2008), "Segmentation of thermal images for non-destructive evaluation of bridge decks", *41*, 395-405.
- ASTM. (2014), Standard Test Method for Detecting Delaminations in Bridge Decks Using Infrared Thermography. ASTM International, West Conshohocken, PA, USA.
- Catbas, F.N., Hiasa, S., Khuc, T., Matsumoto, M. and Mitani, K. (2015), Development, Implementation and Evaluation of Image-based Technologies for Civil Infrastructure Systems. Report Submitted to West Nippon Expressway Company limited (NEXCO-West), Osaka, Japan.
- Cheng, C.C., Cheng, T. and Chiang, C. (2008), "Defect detection of concrete structures using both infrared thermography and elastic waves", *Autom. Constr.*, **18**, 87-92.
- D. Everett, T., Weykamp, P., Capers, H.A., Cox, W.R., Drda, T.S., Lawrence, H., Jensen, P., Juntunen, D.A., Kimball, T. and Washer, G.A. (2008), Bridge Evaluation Quality Assurance in Europe. FHWA, Washington, D.C., FHWA-PL-08-016.
- FHWA. (2013), "Memorandum 'Collection of Element Level Data for National Highway System Bridges'", <<http://www.fhwa.dot.gov/map21/guidance/guideelndhsb.cfm>>.
- FHWA. (2014), "Highway Bridges by State and Highway System 2014", <<http://www.fhwa.dot.gov/bridge/nbi/no10/defbr14.cfm>>.
- FHWA. (2015), "Highway Bridges by Deck Structure Type 2015", <<http://www.fhwa.dot.gov/bridge/nbi/no10/deck15.cfm>> (Apr. 27, 2016).
- FHWA, and FTA. (2014), 2013 Status of the Nation's Highways, Bridges, and Transit: Conditions & Performance.
- FLIR. (2013), The Ultimate Infrared Handbook for R&D Professionals. FLIR AB.
- FLIR. (2015), "Cooled or Uncooled?" FLIR Systems, Inc (As of 2015), <<http://www.flir.com/science/display/?id=65982>>.
- GPO. (2015), "Electronic Code of Federal Regulations", U.S. Government Publishing Office, Subpart C, Title 23, 650.311, <<http://www.ecfr.gov/cgi-bin/text-idx?rgn=div5&node=23:1.0.1.7.28>>.
- Gucunski, N., Kee, S., La, H., Basily, B. and Maher, A. (2015), "Delamination and concrete quality assessment of concrete bridge decks using a fully autonomous RABIT platform", *Struct. Monit. Maint.*, **2**(1), 19-34.
- Gucunski, N., Nazarian, S., Yuan, D. and Kutrubes, D. (2013), Nondestructive Testing to Identify Concrete Bridge Deck Deterioration. Transportation Research Board, SHRP 2 Report S2-R06A-RR-1, Washington, D.C., USA.
- Hashimoto, K. and Akashi, Y. (2010), "Points to consider for photography by infrared cameras with different wavelength detection region", *Proceedings of the 65th JSCE Annual Meeting*, Japan Society of Civil Engineers (JSCE), Sapporo, Japan, VI-160.
- Hiasa, S., Watase, A., Birgul, R., Matsumoto, M., Mitani, K. and Catbas, F.N. (2014). "Utilizing infrared technologies as a non-destructive evaluation for maintenance of concrete structures", *Proceedings of the 4th International Symposium on Life-Cycle Civil Engineering*, IALCCE 2014, CRC Press/Balkema, Leiden, Netherlands.
- Kee, S.H., Oh, T., Popovics, J.S., Arndt, R.W. and Zhu, J. (2012), "Nondestructive bridge deck testing with air-coupled impact-echo and infrared thermography", *J. Bridge Eng.*, **17**(6), 928-939.
- Koch, C., Georgieva, K., Kasireddy, V., Akinci, B. and Fieguth, P. (2015), "A review on computer vision

- based defect detection and condition assessment of concrete and asphalt civil infrastructure”, *Adv. Eng. Informatics*, **29**(2), 196-210.
- Maierhofer, C., Brink, A., Ro, M. and Wiggenshauser, H. (2005), “Quantitative impulse-thermography as non-destructive testing method in civil engineering – Experimental results and numerical simulations”, **19**, 731-737.
- Matsumoto, M., Mitani, K. and Catbas, F.N. (2012). “Bridge assessment methods using image processing and infrared thermography”, 28th US - Japan Bridge Engineering Workshop.
- Matsumoto, M., Mitani, K. and Catbas, F.N. (2015), “NDE for Bridge Assessment using Image Processing and Infrared Thermography The pilot Project”, Transportation Research Board 94th Annual Meeting, TRB, Washington, D.C., USA, No. 15-5620.
- MLIT. (2014), “The present situation of road structures (Bridges)”, Road Bureau, Ministry of Land, Infrastructure, Transport and Tourism, Japan, Tokyo, Japan.
- MLTI. (2014), “Manual for Periodic Bridge Inspection”, Road Bureau, Ministry of Land, Infrastructure, Transport and Tourism, Japan, Tokyo, Japan.
- Nakamura, S., Takaya, S., Maeda, Y., Yamamoto, T. and Miyagawa, T. (2013), “Spalling time prediction by using infrared thermography”, *J. Japan Society of Civil Engineers, Ser. E2 (Materials and Concrete Structures)*, **69**(4), 450-461.
- Nishikawa, T., Hirano, A. and Kamada, E. (2000), “Experimental study on thermography method for external wall removal finished with ceramic tile”, *Architectural Institute of Japan*, **529**, 29-35.
- Oh, T., Kee, S., Arndt, R.W., Popovics, J.S., Asce, M. and Zhu, J. (2013), “Comparison of NDT methods for assessment of a concrete bridge deck”, *J. Eng. Mech. - ASCE*, **139**, 305-314.
- OLRC. (2012), Title 23, United States Code. Office of the Law Revision Counsel of the United States House of Representatives.
- Public Law 112–141. (2012), Moving Ahead for Progress in the 21st Century Act (MAP–21).
- Vaghefi, K., Ahlborn, T. (Tess) M., Harris, D.K. and Brooks, C.N. (2015), “Combined imaging technologies for concrete bridge deck condition assessment”, *J. Perform. Constr. Fac.*, **29**(4), 04014102.
- Washer, G., Fenwick, R. and Bolleni, N. (2009), Development of Hand-held Thermographic Inspection Technologies. Report No. OR10-007.
- Washer, G., Fenwick, R. and Bolleni, N. (2010), “Effects of Solar Loading on Infrared Imaging of Subsurface Features in Concrete”, *J. Bridge Eng.*, **15**, 384-390.
- Watase, A., Birgul, R., Hiasa, S., Matsumoto, M., Mitani, K. and Catbas, F.N. (2015), “Practical identification of favorable time windows for infrared thermography for concrete bridge evaluation”, *Constr. Build. Mater.*, **101**, 1016-1030.
- Wu, L., Mokhtari, S., Nazef, A., Nam, B. and Yun, H. (2014), “Improvement of crack-detection accuracy using a novel crack defragmentation technique in image-based road assessment”, *J. Comput. Civil Eng.*, **30**(1), 04014118.
- Yehia, S., Abudayyeh, O., Nabulsi, S. and Abdelqader, I. (2007), “Detection of common defects in concrete bridge decks using nondestructive evaluation techniques”, *J. Bridge Eng.*, **12**, 215-225.